Modeling and Dynamic Analysis for the Foundation of a Blade-Rotor System

Liang Anyang[1], *Huang Guoyuan*[1], *Zhang Yuetong*[2], *Yue Lin*[1*]

1. College of Mechanical and Electrical Engineering, Nanjing University of Aeronautics and Astronautics, Nanjing 210016, P. R. China;

2. School of Engineering and Informatics, University of Sussex, Brighton BN19RH, United Kingdom

(Received 18 November 2016; revised 2 April 2017; accepted 12 May 2017)

Abstract: In order to achieve the model-based fault monitoring and diagnosis, an accurate model for the rotor system is necessary to locate and quantify faults. Since the dynamic characteristics of a blade-rotor system is influenced by foundation flexibility, the modeling and dynamic analyses on the foundation were sequentially investigated. Firstly, the effect of element size on the model convergence was investigated using the forward difference quotient as the slope of the frequency difference, which found that the model converged when the element size refined to 4 mm. Secondly, a modal analysis and a harmonic response analysis were performed to obtain the dynamic characteristics of the foundation structure. Finally, an optimization to the foundation utilizing an additional stiffener was conducted to reduce the foundation response and make the critical speed far away from the working frequency band of 20—50 Hz.

Key words: finite element model; rotor; modal analysis; harmonic response analysis; foundation

CLC number: TH113; O327 **Document code**: A **Article ID**: 1005-1120(2017)03-0326-07

0 Introduction

In traditional rotor-dynamic analyses, foundation was commonly modeled by lumped mass elements. This representation was easy to analyze using standard rotor-dynamic tools. However, in practice, the dynamic behavior of foundations were much more complex. Only 3D multi-degree-of-freedom models could provide representations close to reality[1-5]. For many applications, the dynamic behavior of foundation usually has a significant effect on resulting rotor response and the locations of critical speeds[6-11]. Therefore, dynamic behavior of foundation has drawn much attention in the rotor-dynamic analyses. Moore[12] et al. performed a rotor-dynamic analysis on a large industrial turbo-compressor including supporting effect. Hong[13] et al. predicted the translation function at the bearing support of an aero-engine and used them in a rotor-dynamic analysis. Santiago[14] et al. presented the results of the dynamic analysis of a power turbine considering turbine frame, gas generator and shims. The generated transfer functions were used to represent the dynamics of these components acting at the rotor bearing locations. Krüger[15] et al. summarized different approaches to include the dynamic characteristics of structures like gas turbine casings and supporting elements in rotor-dynamic analysis.

The primary concern in this study was to perform the modeling and dynamic analysis for the foundation of a blade-rotor as the first step toward the model-based fault monitoring and diagnosis. A 3D finite element(FE) model was generated to determine the natural frequencies, the mode shapes and the dynamic stiffness at bearing pedestals. The subject of this investigation is shown in Fig. 1, which is mainly assembled by a

* Corresponding author, E-mail: yuelinme@nuaa.edu.cn.

How to cite this article: Liang Anyang, Huang Guoyuan, Zhang Yuetong, et al. Modeling and dynamic analysis for the foundation of a blade-rotor system[J]. Trans. Nanjing Univ. Aero. Astro., 2017,34(3):326-332.
http://dx.doi.org/10.16356/j.1005-1120.2017.03.326

casing, a main frame, a supporting structure, two bearing pedestals and four shims. The casing section is a large cylindrical structure, which is bolted to the supporting structure. The two ball bearing pedestals are integrated into the main frame by vertical bolt connections. The main frame configuration is a result of the specific geometric characteristics including a lighter mass and a higher stiffness, which leads to the frame welded by square tubes.

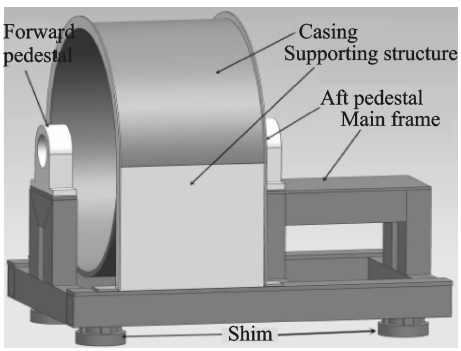

Fig. 1 Foundation structure

1 Foundation Model Constructions

In order to predict the foundation dynamic behavior, a FE model should be developed. The modeling program of a convergent FE model can be organized as the follows:

(1) Perform the inspection and simplification of the model to eliminate the errors generated in geometric modeling.

(2) Create initial models by coarse elements, perform gradual refinement of the mesh, obtain models with different element sizes and conduct modal analysis for these models.

(3) According to the indicator defined by Eq. (1), check the convergence of the model with different element sizes. If it is not convergent, continue to refine the elements.

To describe the convergence of a model quantitatively, the forward difference quotient was utilized, instead of the derivative, as the slope of the frequency difference

$$\Delta f'_{ij} = \left| \frac{\Delta f_{i+1,j} - \Delta f_{i,j}}{y_{i+1} - y_i} \right| \times 10^6 \qquad (1)$$

where $\Delta f_{i,j}$ is the frequency difference percentage of the jth modal of the ith model relative to the most refined model; y_i the number of the ith model's degree of fredom (DOF); $\Delta f'_{ij}$ the slope of the frequency difference curve, which is defined as a percentage of the change in the frequency difference for each additional one million DOF.

Some small features, such as bolt holes and fillets, were not conducive to generate mesh and should be simplified when the FE model was generated. Fig. 1 shows the simplified model. Bonded contact elements were used to represent continuous contacts between different components. Since the complexity of the model, the combination of high order hexahedral elements (20 nodes) and tetrahedral elements (10 nodes) were utilized to generate the mesh. The initial element size was selected as 10 mm and gradually refined to 4 mm. The resulting models are listed in Table 1. The refined model is shown in Fig. 2.

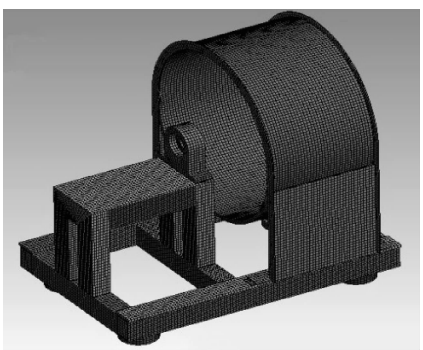

Fig. 2 Initial solid model

All four bottom surfaces were constrained. Modal analyses were performed for these models and the corresponding solving time was shown in Table 1.

Fig. 3(a) shows the relationship between the element size and the number of DOF where x represents the element size. It can be seen that the number of DOF accelerates as the element size becomes smaller. The curve can be fitted by a power function.

Fig. 3(b) presents the relationship between the solving time and the number of DOF where y is the number of degrees of freedom. With the increase of the number of DOF, the solving time increases. The curve can be fitted by a quadratic polynomial function.

Table 1 Model information

Model	Element size / mm	Number of elements	Number of nodes	Number of DOF	Solving time/s
a	10.0	205 746	393 206	1 179 618	618
b	9.0	278 246	519 603	1 558 809	858
c	7.5	380 314	720 824	2 162 472	2 024
d	7.0	433 464	824 012	2 472 036	2 017
e	6.5	600 159	1 136 186	3 408 558	3 262
f	5.0	1 020 683	1 851 396	5 554 188	5 204
g	4.0	1 839 288	3 276 466	9 829 398	8 264

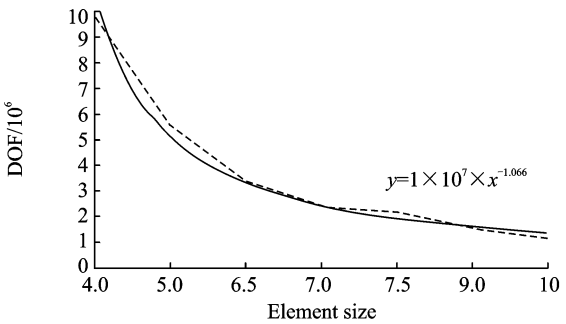

(a) Relationship between the element size and the number of DOF

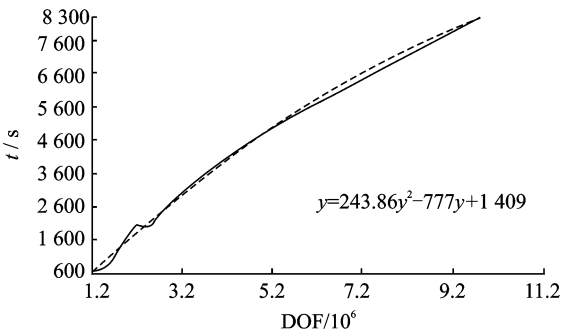

(b) Relationship between the solving time and the number of DOF

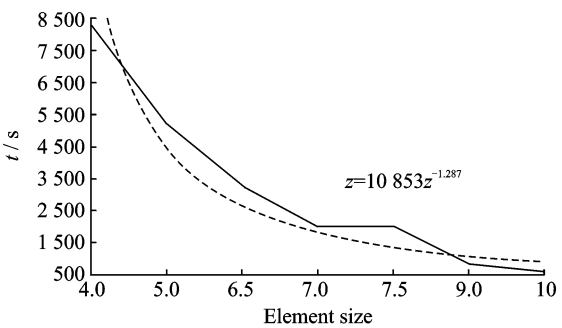

(c) Relationship between the solving time and the element size

Fig. 3 Laws of the convergent model

Fig. 3(c) illustrates the relationship between the solving time and the element size of each model, the curve could be fitted by a power function where z is the solving time. With the gradual refinement of the element, the solving time gradually increases.

The curves of average and maximum frequency difference and the slope of average frequency difference to the most refined model are shown in Fig. 4. In Fig. 4, e_a is the average error

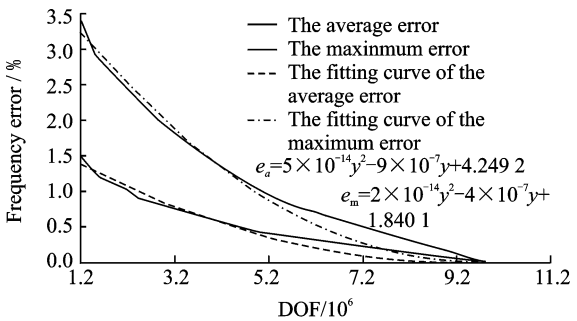

(a) Relationship between the frequency error and the number of DOF

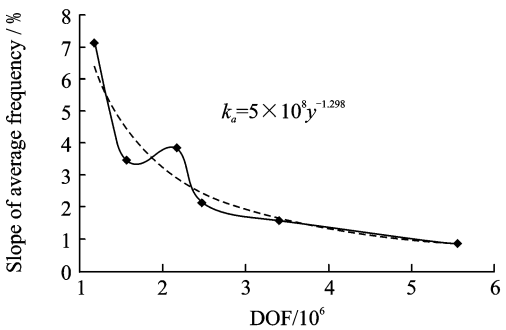

(b) Relationship between the slope of average frequency and the number of DOF

Fig. 4 Frequency difference and slope

of frequency, e_m the maximum error of frequency, and k_a the slope of the frequency average error. It can be seen from Fig. 4 that the frequency difference gradually decreases with the further refinement. When the slope of the average frequency difference is less than 1%, the model converges. So the most refined model can be considered as the convergent model.

2 Modal Analysis

An undamped modal analysis essentially solves the following eigenvalue equation

$$\boldsymbol{M}\ddot{\boldsymbol{x}} + \boldsymbol{K}\boldsymbol{x} = 0 \tag{2}$$

where $\boldsymbol{K}$ and $\boldsymbol{M}$ are the stiffness and the mass matrix respectively, $\boldsymbol{x}$ the displacement vector. The solution of Eq. (2) is

$$\boldsymbol{x} = \varphi_i \cdot \cos\omega_i t \tag{3}$$

where ω_i is the undamped natural frequency of ith mode, $\boldsymbol{\varphi}_i$ the eigenvectors.

A modal analysis was performed for the foundation model to obtain the first six natural frequencies and mode shapes, and the results were shown in Table 2 and Fig. 5, respectively.

Table 2 First six nature frequencies of the initial model

Mode	Frequency /Hz	Mode shape
1	8.996	The 1st bending in XZ plane
2	10.520	Horizontal translation
3	13.868	The 1st torsion in XZ plane
4	22.501	Bending-torsional coupling
5	45.003	Casing the 1st torsion in YZ plane
6	64.804	The 1st torsion in XZ plane

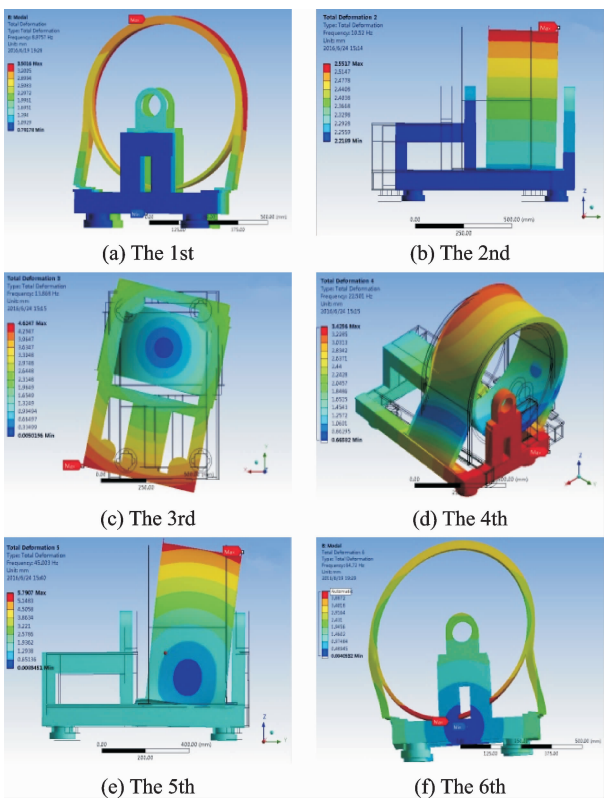

Fig. 5 The first six mode shapes

The modal analysis revealed that if any natural frequencies was in the range of operating speed, a natural mode with motion near the bearing pedestal would ineluctably weaken the support and further reduce the rotor′s critical speeds. The result showed several modes in the frequency range of interest starting with the first bending modes.

3 Harmonic Response Analysis

In order to study the excitation of the steady state centrifugal force caused by an unbalance mass of the rotor and determine the foundation′s dynamic stiffness, a harmonic response was performed at pedestals in orthogonal directions resulting in four independent calculations. From the theory of the theoretical mechanics, the centrifugal force produced by an unbalance mass on a disk can be written as

$$F = mr\omega^2 \tag{4}$$

where F is the centrifugal force; m the eccentric mass; r the eccentric radius and ω the rotating speed of the rotor. The components of F in two coordinate directions at the center of the rotor could be written as follows

$$\begin{cases} F_x = mr\omega^2 \cos\omega t \\ F_z = mr\omega^2 \sin\omega t \end{cases} \tag{5}$$

That is equivalent to two harmonic forces in the center of the disk in two orthogonal directions with the phase difference $\pi/2$. Assuming the eccentric force at the center of the disk is 1 000 N which is arbitrarily chosen but is representative of the force on the rotor and transmitted to the pedestals in the horizontal and the vertical directions, as shown in Fig. 6.

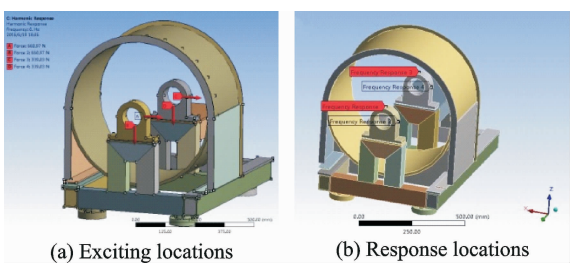

Fig. 6 Harmonic forces and response

Since the modal analysis for the foundation has been performed, the mode superposition method was employed. By the resulted mode shapes vectors, the vibration equation can be decoupled

$$\boldsymbol{M}\ddot{\boldsymbol{x}} + \boldsymbol{K}\boldsymbol{x} = \boldsymbol{f} \tag{6}$$

where $\boldsymbol{f}$ is harmonic force vector. The sub-steps of the harmonic response were set to 200 and the first 40 modes were used from zero to 100 Hz, which cover up twice the frequency range of interest.

The responses in the vertical and the horizontal directions were calculated, as shown in Fig. 7.

The following conclusions can be observed from Fig. 7:

(1) The first four horizontal peaks within 100 Hz correspond to the first four modes. Vertical vibration amplitudes are lower, which indicates that the horizontal stiffness is weaker. A structure optimization will be performed to strengthen the horizontal stiffness and avoid the vibration of the rig at low frequency.

(2) The responses at the forward pedestal in the horizontal and the vertical directions are lower than those produced at the aft pedestal. This conclusion is consistent with the actual rig.

(3) The horizontal and the vertical responses fluctuate significantly with the operating speed. Consequently, it is necessary to consider the dynamic characteristic of foundation in the investigation of the whole rotor system.

(4) There is a discrepancy between the foundation′s rigid assumption and dynamic characters. Dynamic stiffness can better simulate the characteristics and capture the rotor′s critical speed more accurately.

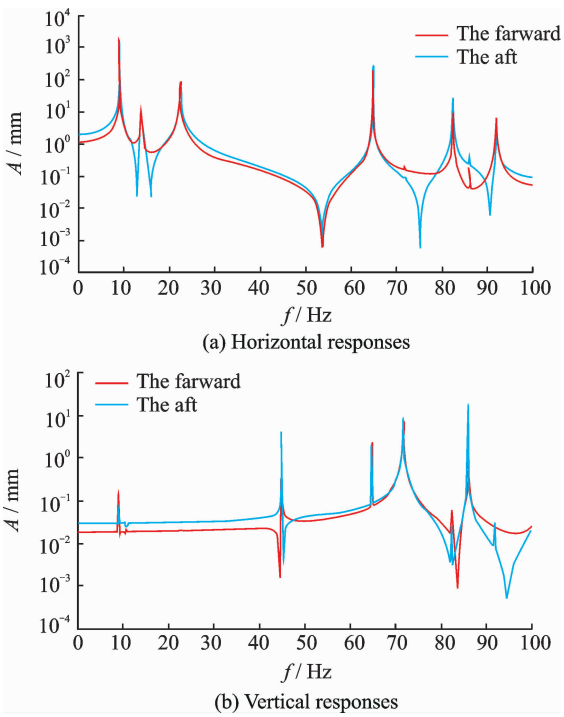

Fig. 7 Harmonic responses

4 Model Optimization

To strengthen the foundation and move the casing modes away from the operating speed, the structure will be optimized. Since the equipment has no contact with the external environment, it is not feasible to strengthen the connection to environment. The optimized design is presented in Fig. 8 utilizing an additional stiffener welded at the support structure. It was identified from the previous mode shapes that a significant amount of bending was occurring at the junction between the casing and the main frame.

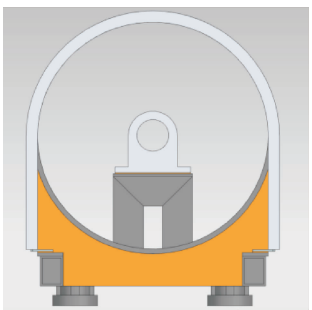

Fig. 8 The optimized design

A modal analysis and a harmonic response analysis of the optimized design were performed in the range 0—100 Hz. The boundary conditions and the element size remained the same. The dynamic stiffness transfer function could be calculated by dividing the excitation force by the response. The horizontal and the vertical dynamic stiffness curves of the original and the optimized models were extracted and comprised in Fig. 9.

It can be drawn from Fig. 9 that the frequency of the first valley has a little change, but the corresponding frequencies of the other valleys and peaks all are improved, especially in the horizontal direction where there is no valley in the range of 15—50 Hz. Wherein the mode corresponding to the second horizontal valley is sufficiently away from the running speed, the response peaks is significantly decreased except the first peak, which indicates that the improvement of the optimization is obvious.

5 Conclusions

The purpose of this investigation was to model and determine the dynamic characteristic of the foundation of a blade-rotor system. Firstly, a

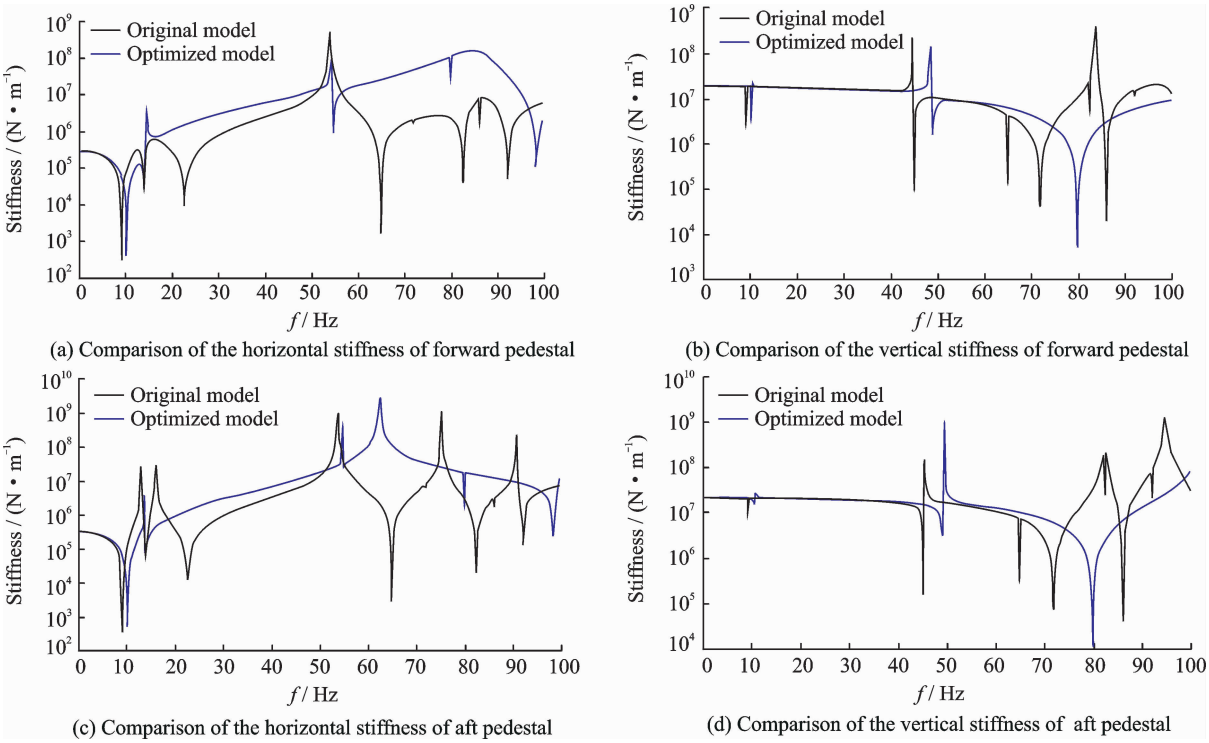

Fig. 9 Comparison of the dynamic stiffness between the optimized design and the original model

method to generate a convergent FE model was investigated. And then a modal analysis and a harmonic response analysis of the convergent foundation model had been performed to obtain the dynamic characteristics. It was found that there was a discrepancy between the foundation's rigid assumption and dynamic characters.

The system contained modes both below and above the designed operating speed. Some of these modes could be excited by the rotor system. Furthermore, the compliance of the foundation due to the presence of these modes caused the second mode in the operating speed. Hence, an optimization was investigated, greatly reduced the dynamic response amplitude of the foundation in the working frequency band and made the critical speed far away from the rotating speed.

Owing to the distinct characteristics of the blade-rotor system, the analytical approach presented in this paper can be utilized to perform rotor-dynamic analysis including dynamic foundation characters. This methodology can discover a potential concern with the critical speeds in the rotor dynamics analysis considering foundation dynamics.

Acknowledgment

This work was supported by the National Key Research and Development Plan (No. 2016YFF0203300).

References:

[1] LAZARUS A, PRABEL B, COMBESCURE D. A 3d finite element model for the vibration analysis of asymmetric rotating machines [J]. Journal of Sound and Vibration, 2010, 329(18):3780-3797.

[2] SYPKAYKIN I T, KELLERER R. Full rotor train modelling approach for assessment of dynamic stresses on rotor and blades due to torsional disturbances [C]//ASME Turbo Expo 2013: Turbine Technical Conference and Exposition. San Antonio, Texas, USA: American Society of Mechanical Engineers, 2013:V07BT31A012-V07BT31A012.

[3] XU Z L, DOU B, FAN X, et al. Last stage blade coupled shaft torsional vibration analysis of 1000 mw steam turbine generator set by a reduced 3d finite element method[C]//ASME Turbo Expo 2014: Turbine Technical Conference and Exposition. Düsseldorf, Germany: American Society of Mechanical Engineers, 2014: V07AT31A029-V07AT31A029.

[4] COMBESCURE D, LAZARUS A. Refined finite element modelling for the vibration analysis of large rotating machines: Application to the gas turbine modular helium reactor power conversion unit[J]. Jour-

nal of Sound and Vibration, 2008, 318(4): 1262-1280.

[5] ZHANG H J, ZHOU C W. Three-dimensional reconstructed finite element model for C/C composites by micro-CT[J]. Trans Nanjing Univ Aero Astro, 2015, 32(6):639-645.

[6] LEES A W, SINHA J K, FRISWELL M I. Model-based identification of rotating machines[J]. Mechanical Systems and Signal Processing, 2009, 23(6): 1884-1893.

[7] YU M, FENG N, HAHN E J. On the identification of the modal parameters for a flexible turbomachinery foundation[C]//ASME Turbo Expo 2012: Turbine Technical Conference and Exposition. Copenhagen, Denmark: American Society of Mechanical Engineers, 2012: 1075-1083.

[8] FENG N, HAHN E. Rotor-model-based identification of foundations in rotating machinery using modal parameters[M]//Vibration Problems ICOVP 2011. Netherlands: Springer Netherlands, 2011: 529-535.

[9] YU M, FENG N, HAHN E J. An equation decoupling approach to identify the equivalent foundation in rotating machinery using modal parameters[J]. Journal of Sound and Vibration, 2016, 365: 182-198.

[10] CHEN Xi, LIAO Mingfu, LIU Zhanchi, et al. Modal balancing method for flexible rotors with elastic supports[J]. Journal of Nanjing University of Aeronautics and Astronautics, 2016, 48(3): 402-409. (in Chinese)

[11] KRAMER E. Dynamics of rotors and foundations[M]. Heidelberg, Germany: Springer Science & Business Media, 2013.

[12] MOORE J J, VANNINI G, Camatti M, et al. Rotordynamic analysis of a large industrial turbocompressor including finite element substructure modeling[J]. Journal of Engineering for Gas Turbines and Power, 2010, 132(8): 082401.

[13] HONG J, CHEN M, LIU S. Application of whole engine finite element models in aero-engine rotordynamic simulation analysis[C]//ASME Turbo Expo 2007: Power for Land, Sea, and Air. [s. l.]: American Society of Mechanical Engineers, 2007: 771-778.

[14] DE SANTIAGO O, ABRAHAM E. Rotordynamic analysis of a power turbine including support flexibility affects[C]//ASME Turbo Expo 2008: Power for Land, Sea, and Air. [s. l.]: American Society of Mechanical Engineers, 2008: 1173-1181.

[15] KRüGER T D, LIBERATORE S, KNOPF E, et al. Consideration of complex support structure dynamics in rotordynamic assessments[C]//ASME Turbo Expo 2013: Turbine Technical Conference and Exposition. San Antonio, Texas, USA: American Society of Mechanical Engineers, 2013: V07AT29A016-V07AT29A016.

Mr. **Liang Anyang** is Ph. D. candidate from Nanjing University of Aeronautic and Aestronautics. His main research interests are in the areas of rotor dynamic, finite element model updating and condition monitoring and fault diagnosis of large rotating machines.

Mr. **Huang Guoyuan** is a postgraduate from Nanjing University of Aeronautic and Aestronautics. His main research interests are in the areas of signal acquisition and structure health monitoring.

Mr. **Zhang Yuetong** is a postgraduate from University of Sussex. His main research interests are in the areas of structure health monitoring.

Prof. **Yue Lin** received Ph. D. degree in machine design and theory from Nanjing University of Aeronautic and Aestronautics. Nanjing, China, in 2003. From Jan. to Apr. 2004, she had worked as a visiting scholar in the school of Industrial & Manufacturing Science (SIMS), Cranfield University, United Kingdom. Her main research interests are in the areas of vibration, impact, noise and condition monitoring and fault diagnosis of large rotating machines.

(Executive Editor: Zhang Bei)